Role of Alveolar Macrophages in Respiratory Transmission of Visna/Maedi Virus

JOURNAL OF VIROLOGY, Feb. 2008, p. 1526–1536 Vol. 82, No. 3
0022-538X/08/$08.00+0 doi:10.1128/JVI.02148-07

Role of Alveolar Macrophages in Respiratory Transmission of Visna/Maedi Virus▽

Tom N. McNeilly,* Alison Baker, Jeremy K. Brown, David Collie, Gerry MacLachlan, Susan M. Rhind, and Gordon D. Harkiss

Royal (Dick) School of Veterinary Studies, University of Edinburgh, Easter Bush Veterinary Centre, Easter Bush, Midlothian EH25 9RG, United Kingdom

Received 1 October 2007/Accepted 13 November 2007

A major route of transmission of *Visna/maedi virus* (VMV), an ovine lentivirus, is thought to be via the respiratory tract, by inhalation of either cell-free or cell-associated virus. In previous studies, we have shown that infection via the lower respiratory tract is much more efficient than via upper respiratory tissues (T. N. McNeilly, P. Tennant, L. Lujan, M. Perez, and G. D. Harkiss, J. Gen. Virol. 88:670–679, 2007). Alveolar macrophages (AMs) are prime candidates for the initial uptake of virus in the lower lung, given their in vivo tropism for VMV, abundant numbers, location within the airways, and role in VMV-induced inflammation. Furthermore, AMs are the most likely cell type involved in the transmission of cell-associated virus. In this study, we use an experimental in vivo infection model that allowed the infection of specific segments of the ovine lung. We demonstrate that resident AMs are capable of VMV uptake in vivo and that this infection is associated with a specific up-regulation of AM granulocyte-macrophage colony-stimulating factor mRNA expression ($P < 0.05$) and an increase in bronchoalveolar lymphocyte numbers ($P < 0.05$), but not a generalized inflammatory response 7 days postinfection. We also demonstrate that both autologous and heterologous VMV-infected AMs are capable of transmitting virus after lower, but not upper, respiratory tract instillation and that this transfer of virus appears not to involve the direct migration of virus-infected AMs from the airspace. These results suggest that virus is transferred from AMs into the body via an intermediate route. The results also suggest that the inhalation of infected AMs represents an additional mechanism of virus transmission.

Visna/maedi virus (VMV) is a member of the lentivirus subgroup of retroviruses that cause lymphoid interstitial pneumonia, encephalitis, arthritis, and mastitis in sheep (40, 41). The main routes of transmission of VMV are thought to be through the ingestion of infected colostrum and/or milk or through the inhalation of infected respiratory secretions (6, 34). We recently have demonstrated that a major route of respiratory transmission is likely via the uptake of cell-free VMV in the lower respiratory tract (33), although the initial target cells for cell-free VMV at this site were not identified.

It is known that VMV exhibits strong tropism for alveolar macrophages (AMs) in vivo in naturally infected sheep (7, 9, 18, 30) and is present in AMs following experimental infection from 11 days after lung instillation (19, 42). In addition, AMs are present in large numbers within the lower lung airspace. Consequently, AMs represent a likely initial target for VMV uptake in the lower respiratory tract and therefore may play a key role in the respiratory transmission of VMV.

Assuming AMs play a role in respiratory transmission of VMV, virus taken up by resident AMs must be transmitted from these cells within the lung airspace into the body. As yet there is no information regarding the transfer of virus from VMV-infected AMs in the airspace to adjacent lung tissue. Transfer of virus from infected AMs also may be relevant with regard to heterologous cell-associated virus transmission, as it is possible that respiratory transmission is mediated by the inhalation of both cell-free and cell-associated VMV derived from infected individuals. However, as yet there is no direct evidence that cell-associated virus transmission occurs between sheep.

If virus transfer occurs from VMV-infected AMs in the airspace entering into the body, it is likely to involve the infection of the draining lymph nodes, which are thought to be important initial sites of infection (5). This transfer may involve an indirect route or may occur by direct migration of infected AMs to the lymph node, as there is evidence to suggest that AMs are capable of migrating from the alveolar space into the regional lymphoid tissue (12, 23, 27).

AMs also have been implicated as the main cell type involved in VMV-induced lung inflammation, primarily by the dysregulation of cytokine gene expression and subsequent recruitment of inflammatory cells (29, 50). It is possible that AMs mediate a similar inflammatory response during early VMV infection in vivo, as suggested by the observed up-regulation of interleukin-8 (IL-8) expression by AMs within 48 h of in vitro infection (28). This may have implications for the enhancement of virus uptake, as a number of proinflammatory cytokines have been shown to enhance VMV replication in AMs and other macrophages in vitro (15, 50), and generalized inflammation is likely to result in the recruitment of VMV target cells, namely, macrophages and dendritic cells (DCs) (7, 36).

In this study, we investigated the role of AMs in initial VMV uptake using a segmental lung model system. We demonstrate that AMs are capable of the uptake of cell-free virus in vivo and that early VMV infection is associated with a specific

* Corresponding author. Present address: Moredun Research Institute, Pentlands Science Park, Bush Loan, Penicuik EH26 0PZ, United Kingdom. Phone: 44 (0) 131 445 5111. Fax: 44 (0) 131 445 6111. E-mail: Tom.McNeilly@Moredun.ac.uk.

▽ Published ahead of print on 28 November 2007.

up-regulation of AM granulocyte-macrophage colony-stimulating factor (GM-CSF) mRNA expression in the absence of a generalized inflammatory response. Furthermore, we demonstrate that both autologous and heterologous VMV-infected AMs are capable of transmitting virus into the body after instillation into the lower lung, and that the transfer of virus from AMs in the lower lung to regional lymph nodes appears not to involve AM migration.

MATERIALS AND METHODS

Virus propagation and titration. Low-passage VMV strain EV1 (38) was propagated and titrated on ovine skin cells (OSCs) as described previously (33). Mock-infected medium controls were generated by culturing the same OSCs as those used for virus propagation, but without the addition of virus. Supernatants were collected on the same day as viral supernatants and processed identically.

BAL. Bronchoalveolar lavage (BAL) was performed either under general anesthesia or at postmortem as described previously (11). Lavage fluid subsequently was centrifuged at 400 × *g* for 7 min, and the resultant cell pellets were resuspended in sterile phosphate-buffered saline (PBS). Cells were counted using a Neubauer hemocytometer before cytocentrifuge preparation, AM purification, and VMV infection.

Differential cytology of BAL cells. Cytocentrifuge slides were stained using Leishman's stain, and differential cell counting was performed on 500 cells. Cells were classified as macrophages, neutrophils, lymphocytes, eosinophils, mast cells, or other cells according to standard morphological criteria. Total numbers of BAL cells/milliliter of BAL fluid and the percentage of each cell type within the BAL cell population were compared to previously published normal limits (11).

Purification of AMs and RNA extraction. The purification of AMs was based on a procedure described previously (28, 50) that relies on the preferential adherence of macrophage populations to tissue culture flasks. After pelleting and counting BAL cells, cells were resuspended in 7 ml RMPI 1640 medium (Invitrogen, Paisley, United Kingdom) containing 10% fetal calf serum (FCS), 2 mM L-glutamine, 50 μg/ml penicillin, 50 μg/ml streptomycin, 2 μg/ml amphotericin B, and 0.05 M β-mercaptoethanol and were seeded into 25-cm^2 tissue culture flasks. After 2 h of incubation at 37°C with 5% CO_2, nonadherent cells were removed by washing with PBS. This purification method consistently resulted in 96 to 98% pure populations of AMs, as determined by morphological assessment and CD14 staining of cytocentrifuge preparations during preliminary experiments. Adherent cells were trypsinized, washed once with 7 ml fresh medium, and resuspended in 350 μl RLT buffer (Qiagen, Crawley, United Kingdom) containing 1% (vol/vol) β-mercaptoethanol. Total RNA extraction then was carried out using the RNeasy mini kit (Qiagen), including on-the-column digestion of DNA with RNase-free DNase (Qiagen), by following the manufacturer's instructions for animal cells.

RNA extraction from animal tissue. Samples of either lung parenchyma (1 cm^3) or lymph node (0.5 cm^3) were collected postmortem and stored in RNA*later* (Qiagen) at −80°C prior to RNA extraction using the Fastprep cell disrupter system (Bio 101 Thermoelectron; Qbiogene, Cambridge, United Kingdom). Samples of lung parenchyma (100 mg) or lymph node (20 mg) in 1 ml RLT buffer (Qiagen) containing 1% (vol/vol) β-mercaptoethanol were placed in a 2-ml Eppendorf tube containing lysis matrix D (Qbiogene) and pulsed in a Fastprep machine for 40 s. Supernatants then were passed through a Qiashredder column (Qiagen), and total RNA was extracted using the RNeasy mini kit, including on-the-column digestion of DNA with RNase-free DNase (Qiagen), by following the manufacturer's instructions for animal tissues.

Real-time RT-PCR quantitation of AM cytokine gene expression and VMV *gag* RNA. The relative quantitation of cytokine gene expression and VMV RNA by two-step real-time reverse transcription-PCR (RT-PCR) was performed using the standard curve method. To generate VMV *gag* RNA standard curves, serial dilutions of plasmid pDS1-*gag* containing the whole VMV strain EV1 *gag* gene (provided by Heide Niesalla, University of Edinburgh) were amplified. To generate plasmids for cytokine and glyceraldehyde 3-phosphate dehydrogenase (GAPDH) standard curves, RNA was extracted from in vitro VMV-infected AMs and cDNA was constructed using Superscript II (Invitrogen) and anchored oligo(dT) primers (Sigma) according to the manufacturer's instructions. External primers spanning 300 to 500 bp were used to generate primary PCR products. PCR was carried out with Hot *Taq* DNA polymerase (Biogene, Kimbolton, United Kingdom) according to the manufacturer's recommendations and using 3 μl cDNA and 25 pmol of each primer. Primer sequences and annealing temperatures are shown in Table 1.

PCR products were purified using the S.N.A.P. UV-free gel purification kit (Invitrogen) and subsequently cloned into the sequencing vector pCR2.1-TOPO (Invitrogen) according to the manufacturer's instructions. Aliquots of each plasmid were sequenced to confirm the presence of the correct insert.

Real-time PCR was performed on cDNA samples using a RotorGene 3000 real-time thermal cycler (Corbett Research, Sydney, Australia) and the appropriate internal primer sets (Table 1). Cycling was performed in 20-μl reaction volumes containing 1 μl cDNA, 10 μl of 2× Quantitect SYBR green PCR master mix (Qiagen), and 0.5 μM of each primer. Thermal cycling parameters involved a 15-min preincubation at 95°C followed by 40 cycles of denaturation at 94°C for 20 s, primer annealing at 52 to 57°C for 20 s, and extension at 72°C for 20 s. Fluorescence data acquisition was performed after each extension step.

Following amplification, a plot of the fluorescence versus the cycle number was generated. The threshold value for each sample was calculated automatically by the RotorGene software (version 5.10) using the fit-point method. Serial 1:10 dilutions of plasmid containing the gene of interest ranging from 10^8 to 10^2 copies per μl were run in parallel with each series of samples, allowing the automatic generation of a standard curve by the RotorGene software. The correlation coefficients of standard curves were between 0.98 and 0.99, and PCR efficiencies calculated from the slopes were >90%. The number of copies per microliter of sample then was calculated for each sample and results were normalized to GAPDH, the expression of which had previously been shown to be unaffected by VMV infection. Standards were run in triplicate, and samples were run in duplicate. Melting curve analysis was performed at the end of each PCR run to verify the specificity of the PCR product.

Immunocytochemistry and histopathology. Selected lung lobes were inflated with a 1:1 mixture of OCT compound (Tissue-Tek; Sakura-Finetek, Zoeterwoude, The Netherlands) before being cut into 1-cm^3 blocks and snap-frozen in isopentane-dry ice. Tissue sections were cut to 6 μm thick, mounted on poly-L-lysine-coated slides (BDH, Poole, United Kingdom), and stored at −80°C prior to use.

Immunocytochemical staining was performed on tissue sections and cytocentrifuge slides as previously described (32) using the EnVision Plus HRP system (DakoCytomation, Ely, United Kingdom). Details of monoclonal antibodies (MAbs) used in this study are provided in Table 2. Cell counts were expressed as the number of positively stained cells per millimeter of bronchiolar epithelium for airways and the number of positively stained cells per square millimeter of lung tissue for lung parenchyma (determined by stereology).

For histopathological analysis, appropriate tissue sections were stained with hematoxylin and eosin. Samples were analyzed blindly by a trained histopathologist, and descriptive qualitative comments on each slide were provided.

Ex vivo infection of AMs with VMV. Immediately after collection, BAL cells were incubated in RMPI 1640 medium (Invitrogen) containing 2 mM L-glutamine and 10% FCS with 1 50% tissue culture infectious dose ($TCID_{50}$)/cell VMV strain EV1 in VueLife 7 tissue culture bags (Cellgenix, Freiburg, Germany) for 2 h. Cell suspensions then were centrifuged at 400 × *g* for 5 min and resuspended in 25 ml PBS. Cell pellets were washed a further five times in PBS before finally being resuspended in an appropriate volume of PBS. Prior to instillation, viable cell counts were performed using trypan blue exclusion, and differential cytology revealed cell populations to be between 90 and 95% AMs. Aliquots of the last wash were stored at −80°C for subsequent virus titration to confirm the absence of cell-free virus.

Respiratory tract instillation of cell-free VMV and VMV-infected AMs. For upper respiratory tract instillations of VMV-infected AMs, 1×10^6 cells were resuspended in 2 ml PBS, and 1 ml was instilled into each nostril using a modified 8F portex intravenous catheter (Sims Portex Ltd., Hythe, United Kingdom), which resulted in the exposure of the nasal cavity and nasopharynx to instillates, and was shown not to affect AM viability.

Lower respiratory tract instillations of free virus or virus-infected AMs were performed under general anesthesia and delivered via a 21-gauge polyethylene catheter inserted into the lateral channel of a flexible fiber optic bronchoscope (5.3 mm outer diameter) (model FG-16X; Pentax, Englewood, CO). For instillations of cell-free VMV, 2-ml volumes containing 1×10^6 $TCID_{50}$ VMV were delivered endoscopically into the left cardiac lung lobe. At the same time, an equivalent volume of mock-infected medium control was instilled into a right cardiac lung lobe. For the instillation of VMV-infected AMs, 1×10^6 cells in 2 ml PBS were delivered into either the left or right cardiac lung lobes as required, and donor AMs were harvested from either the right or left caudodorsal lobe.

Detection of VMV-specific provirus, transcripts, and serum antibodies. VMV proviral *gag* DNA in peripheral blood mononuclear cells (PBMCs) was detected by seminested PCR (snPCR) as described previously (33). Spliced viral transcripts of *rev* and *env* genes were detected by RT-snPCR.

For the detection of *rev* gene transcripts, snPCR of cDNA samples was per-

TABLE 1. Primer sequences and annealing temperatures for real-time PCR assays

Gene product (reference)	GenBank accession no.	Primer type	Primer sequence[b] (5′→3′)	Product size (bp)	Annealing temp (°C)
GAPDH[a]	AF030943	External	F, AAG GCA GAG AAC GGG AAG R, AGT GAT GGC GTG GAC AGT	366	55
		Internal	F, GGT GAT GCT GGT GCT GAG TA R, TCA TAA GTC CCT CCA CGA TG	265	57
GM-CSF[a]	NM_001009805	External	F, GCC TGC TTC ACT TCT GGA C R, GCT TCT CCT GGG CAC TGT	425	55
		Internal	F, GAT GGA TGA AAC AGT AGA AGT CG R, CAG CAG TCA AAG GGA ATG AT	261	57
Tumor necrosis factor alpha[a]	X55152	External	F, TCC TTG GTG ATG GTT GGT R, CAC TGA CGG GCT TTA CCT C	525	58
		Internal	F, GAA TAC CTG GAC TAT GCC GA R, CCT CAC TTC CCT ACA TCC CT	238	57
Tumor growth factor β1 (49)	NM_001009400	External	F, GCC CTG GAC ACC AAC TAC TG R, TCA GCT GCA CTT GCA GGA G	338	61
		Internal	F, GAA CTG CTG TGT TCG TCA GC R, GGT TGT GCT GGT TGT ACA GG	169	55
IL-1β[a]	NM_001009465	External	F, CTG TGT TCT TCC CTT CCC TT R, CAA AAA TCC CTG GTG CTG	518	55
		Internal	F, CCT TGG GTA TCA GGG ACA A R, TGC GTA TGG CTT TCT TTA GG	317	57
IL-6 (14)	NM_001009392	External	F, GCT TCC AAT CTG GGT TCA R, CCA CAA TCA TGG GAG CCG	347	55
		Internal	F, TCC AGA ACG AGT TTG AGG R, CAT CCG AAT AGC TCT CAG	236	52
IL-8	NM_001009401	External	F, GAA GTC CTC TGG GAC AGC AG R, TTG GAA GCA ATG GAA AAA GG	429	55
		Internal	F, ATG AGT ACA GAA CTT CGA R, TCA TGG ATC TTG CTT CTC	222	55
IL-10 (14)	NM_001009327	External	F, AGC TGT ACC CAC TTC CCA R, GAA AAC GAT GAC AGC GCC	305	55
		Internal	F, TGA AGG ACC AAC TGA ACA GC R, TTC ACG TGC TCC TTG ATG TC	160	55
IL-12p40[a]	AF209435	External	F, CTG CTG CTT TTG ACA CTG AA R, CTG GTT TTC CCT GGT TTT G	452	54
		Internal	F, TCA GAC CAG AGC AGT GAG GT R, GCA GGT GAA GTG TCC AGA AT	243	57
IL-18[a]	NM_001009263	External	F, TCA GAT CAC GTT TCC TCT CC R, GAT GGT TAC AGC CAG ACC TC	348	55
		Internal	F, GAG CAC AGG CAT AAA GAT GG R, TGA ACA GTC AGA ATC AGG CAT A	241	57
VMV Gag	S51392	Internal	F, TAG AGA CAT GGC GAA GCA AGG CT R, TCC TGC TTG CAA ATT TAC AAT AGG	462	55

[a] Primers were kindly donated by Katie Matthews, University of Edinburgh.
[b] F, forward (sense) primer; R, reverse (antisense) primer.

formed using the first-round primer pair *rev* 1 (sense, CAG AGT AAC CTG GAC AGA CA) and *rev* 3 (antisense, TAT CTG GGT AAA AGT GCG CC) and the second-round primer pair *rev* 1 and *rev* 2 (antisense, GTT TTT CCT CGA GGT CCA CA). Both the first- and second-round primer pairs spanned the *rev* internal splice site of VMV strain EV1 (nucleotide position 6129; accession no. S51392) and generated PCR products of 272 and 189 bp, respectively. RT-snPCR detection of *env* gene transcripts was performed using the first-round primer pair *env* 1 (sense, AGA GAA GCG ACG AAA GGA CC) and *env* 3 (antisense, CCA TTT TTC ACA TGG TTC CC) and the second-round primer pair *env* 1 and *env* 2 (antisense, TAC CTG TTA CCA AGC CCT GC). The first- and second-round primer pairs spanned the major splice donor site of EV1 (nucleotide position 319; accession no. S51392). Due to alternative splicing at the 5′ end of the *env* gene transcripts, two PCR products were generated for both first-round (354 and 399 bp) and second-round (263 and 308 bp) reactions (accession nos. AM501483 and AM501484, respectively).

PCR was carried out using Hot *Taq* DNA polymerase (Biogene) and 25 pmol of each primer. Five microliters of cDNA was added to first-round reactions, and a 3-μl aliquot from the first round of PCR was used in the second-round reaction. First- and second-round reactions involved 15 and 35 cycles of amplification, respectively.

VMV-specific antibodies in serum were detected using a commercial enzyme-linked immunosorbent assay (ELISA) kit (ELITEST-MVV/CAEV; Hyphen Biomed, Neuville sur Oise, France) (37).

Fluorescent labeling of VMV-infected AMs with PKH26 dye. Cells were fluorescently labeled using a PKH26 red fluorescence cell-linker kit (Sigma, St. Louis, MO) according to the manufacturer's instructions. Prior to the use of labeled cells, viable cell counts were performed using trypan blue exclusion, and a cytocentrifuge preparation of an aliquot of the stained cells was analyzed using

TABLE 2. Details of MAbs used in immunocytochemical staining[c]

MAb	Specificity (reference)	Cellular expression (reference)
SW 73.2[a]	MHC II	DCs, B cells, activated T cells, macrophages (25)
CC20[b]	CD1b	DCs including RTDCs, cortical thymoctes (26, 32)
17D[b]	CD4	T-helper cells (31)
SBU-T8[b]	CD8	T-cytotoxic cells (31)
VPM67[a]	CD14	Monocytes, macrophages (21)
VPM70	VMV p25 capsid protein (35)	NA

[a] Kindly donated by Professor John Hopkins, University of Edinburgh.
[b] Kindly donated by Ian Anderson, Moredun Research Institute.
[c] CD, cluster designation; MHC II, major histocompatibility complex class II; NA, not applicable.

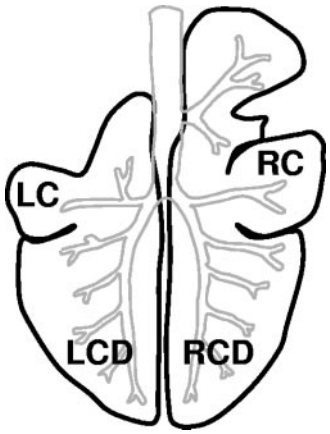

FIG. 1. Diagram of the ovine lung indicating the location of lung segments used for the delivery of multiple treatments and the provision of control samples within the same sheep. LC, left cardiac lung lobe; RC, right cardiac lung lobe; LCD, left caudodorsal lung lobe; RCD, right caudodorsal lung lobe.

an MPV II fluorescence microscope (Leitz, Wetzlar, Germany) to assess the intensity and uniformity of staining.

Detection of PKH26-labeled cells. The detection of PKH26-labeled cells after in vivo lung instillation was performed using fluorescence microscopy. At postmortem, BAL was performed on appropriate lung segments, and samples of lung tissue and lymph nodes were collected. Cytocentrifuge slides of BAL cells and sections of lung tissue and lymph nodes were fixed for 5 min in 4% paraformaldehyde in PBS at room temperature. Slides were washed twice in PBS for 3 min each before incubation in 0.5 M glycine in PBS for 5 min at room temperature. After two further PBS washes, slides were incubated in SYBR green (Roche, Mannheim, Germany) diluted 1:20,000 in PBS for 5 min. After a final PBS wash, slides were mounted in Mowiol mounting medium (Calbiochem-Novabiochem, San Diego, CA) and allowed to set for 1 h at room temperature before microscopic analysis using an MPV II fluorescence microscope (Leitz). For cytocentrifuge preparations, a total of 1,000 cells was counted, and the number of PKH26-positive cells was recorded. For tissue samples, a total of 10 sections cut at 100-μm intervals was analyzed per sample, and the location of positive cells was recorded.

Sheep. Six Blackface ewes were used to assess the in vivo uptake of cell-free VMV by AMs and subsequent lung inflammatory responses. Suffolk-cross ewes were used to assess both the infectivity of AM-associated VMV in vivo ($n = 7$) and the migration of VMV-infected AMs after lower lung instillation ($n = 7$). All sheep were commercially sourced, determined to be free from VMV provirus, and seronegative for VMV-specific antibodies prior to use. All experimental procedures involving animals were approved by The University of Edinburgh's Biological Services Ethical Review Committee and were performed under license as required by the United Kingdom's Animals (Scientific procedures) Act 1986.

Statistical analysis. Data were analyzed for normality of distribution using the Kolmogorov-Smirnov and Anderson-Darling tests. Real-time PCR data, BAL cytology, and immunocytochemical cell counts all were normally distributed, and therefore statistical analyses were performed using paired t tests. P values of <0.05 were considered significant.

RESULTS

Uptake of cell-free VMV by AMs in vivo. The lung was classified into various anatomical segments, as shown in Fig. 1, to allow multiple treatments within the same animal and to provide within-animal control samples. This segmental approach for VMV lung instillation has been described previously (17, 42). To evaluate the uptake of cell-free VMV by resident lung AMs, 1×10^6 $TCID_{50}$ of VMV were instilled into the left cardiac lung lobe of six sheep, and at the same time an equivalent volume of mock-infected medium was instilled into

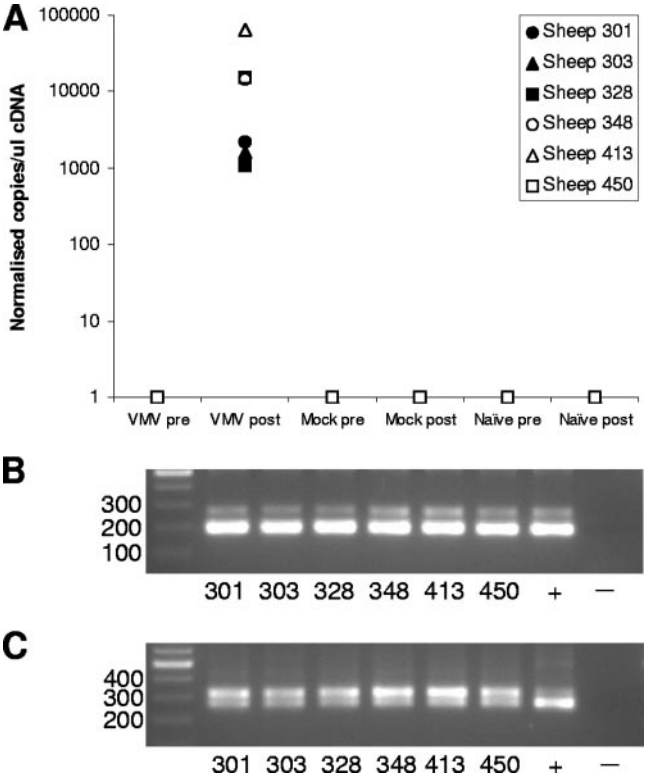

FIG. 2. PCR detection of VMV RNA in purified AMs obtained from VMV-treated (VMV), mock-treated (Mock), and untreated (Naïve) lung lobes of six adult Blackface ewes 7 days pre- and postinstillation. (A) Detection of VMV *gag* RNA in AMs by real-time RT-PCR. (B) Detection of VMV *rev* transcripts in AMs obtained from virus-treated lung lobes by RT-snPCR. (C) Detection of VMV *env* transcripts in AMs obtained from virus-treated lung lobes by RT-snPCR. pre, preinstillation; post, postinstillation; +, positive control (cDNA from in vitro-infected OSCs); −, negative control.

the right cardiac lobe. AMs from virus-treated, mock-treated lung lobes and a naive lung lobe (right caudodorsal) were harvested by BAL 7 days postinstillation. Following AM purification, cells were analyzed for the presence of VMV RNA by real-time RT-PCR. Baseline AMs harvested from the relevant lung lobes 7 days preinstillation also were analyzed. Viral *gag* RNA was detected in AMs from virus-treated lung lobes in all six sheep, with values ranging from 1,000 to 66,000 copies/μl cDNA. No viral RNA was detected in AMs purified from mock-infected or nontreated control lung lobes or in AMs purified prior to virus instillation (Fig. 2A). GAPDH was detected in all cDNA samples, indicating that RNA extraction and RT were successful for all samples analyzed (data not shown). No dissemination of virus from the virus-treated lung lobes to control lobes was observed 7 days postinfection, validating the segmental approach to VMV lung instillation used in this study.

Spliced viral gene transcripts of both *rev* and *env* genes (expressed early and late in the VMV life cycle, respectively [39]) were detected by RT-snPCR of AMs obtained from virus-treated lung lobes in all sheep. For *rev* PCRs, two PCR products of approximately 190 and 270 bp were generated in all AM samples and positive control cDNA (generated from in vitro-

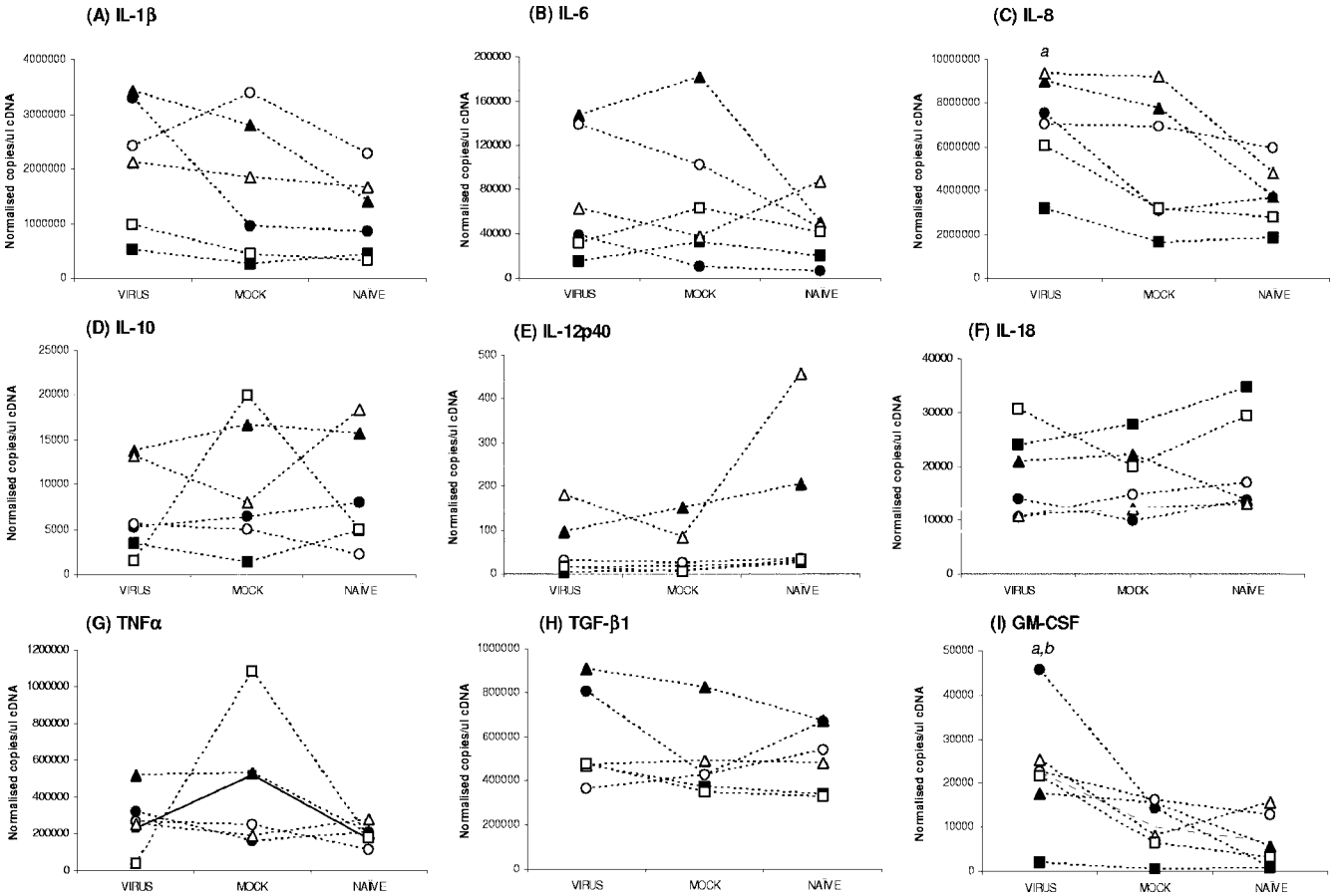

FIG. 3. Real-time RT-PCR analysis of cytokine mRNA expression in AMs obtained from VMV-treated (VIRUS), mock-virus treated (MOCK), and untreated (NAÏVE) lung lobes of six adult Blackface ewes 7 days postinstillation. Lines connect measurements in the three different lung lobes in the same sheep. *a*, significant difference compared to the value for untreated lung lobes ($P < 0.05$; paired *t* test); *b*, significant difference compared to the value for mock-treated lung lobes ($P < 0.05$; paired *t* test). Symbols: ●, sheep 301; ▲, sheep 303; ■, sheep 328; ○, sheep 348; △, sheep 413; □, sheep 450.

infected OSCs), corresponding to first- and second-round PCR products (Fig. 2B). Interestingly, *env* PCR analysis of AM cDNA resulted in the generation of two PCR products of 263 and 308 bp in size, whereas the amplification of positive control cDNA produced only the smaller *env* PCR product (Fig. 2C). The two *env* transcripts differed by a 45-bp insert located 3′ to the RNA polymerase II binding site and 5′ to the start of translation (data not shown). Immunocytochemistry failed to detect any viral capsid protein expression. Therefore, it is concluded that AMs are capable of the uptake of cell-free VMV in vivo and support virus replication to at least the level of late viral gene transcription.

Assessment of lung inflammatory responses during early VMV infection in vivo. We hypothesized that local inflammatory responses influence initial virus uptake within the lung, either by modulating virus replication within infected cells or by the recruitment of VMV target cells. Following lower lung instillation of 1×10^6 $TCID_{50}$ of cell-free VMV strain EV1, virus was detected in the blood from 2 to 3 weeks postinstillation (33). Therefore, key events involved in virus uptake from the lung airspace are likely to occur during this initial 2- to 3-week period. For this reason, lung inflammation was assessed at 7 days postinstillation, a time point within the previremic stage of VMV infection.

BAL cells and lung tissue samples from virus-treated, mock-treated, and naïve lung lobes generated from the above experiment were analyzed using a combination of real-time RT-PCR, cytology of BAL cells, histopathology, and immunocytochemistry. BAL cell populations were analyzed 7 days pretreatment and 7 days posttreatment; lung tissue was analyzed at 7 days posttreatment. As no dissemination of virus from virus-treated lung lobes was evident at 7 days posttreatment, a direct comparison between inflammatory responses in virus-treated and control lung lobes could be made for each individual sheep, thus allowing paired statistical analyses of data.

Real-time RT-PCR analysis of cytokine mRNA expression was performed on purified AM populations obtained from VMV-treated, mock-treated, and naïve lung lobes. The results of the analysis of AM cytokine mRNA expression 7 days posttreatment are shown in Fig. 3. The level of GM-CSF mRNA expression was significantly up-regulated in AMs obtained from virus-treated lung lobes compared to those of AMs from both mock-treated ($P < 0.05$) and naïve lung lobes ($P < 0.05$) 7 days postinstillation (Fig. 3I). A significant increase in IL-8

TABLE 3. Summary of weekly PCR and ELISA results for detection of VMV infection after in vivo instillation of VMV-infected AM

Sheep no.	Instillation route[a]	VMV-AM prepn[a]	Titer of VMV-AM in vitro ($TCID_{50}$/ml)[b] on day:		Wks to PBMC being PCR positive[c]	Wks to serum being ELISA positive[c]
			0 (last wash)	7 (supernatant)		
1675	Lower lung	Autologous (A)	0	1.1×10^5	2	2
1676	Lower lung	Heterologous (A)	0	1.1×10^5	2	3
1677	Lower lung	Autologous (B)	0	2.0×10^5	2	7
1678	Lower lung	Heterologous (B)	0	2.0×10^5	2	3
5797	Lower lung	Heterologous (C)	0	4.0×10^6	11	17
5798	Nasal	Heterologous (C)	0	4.0×10^6	>26	>26
5800	Nasal	Heterologous (C)	0	4.0×10^6	>26	>26

[a] AMs infected with VMV ex vivo were instilled into the left cardiac lung lobe (lower lung) or upper respiratory tract (nasal) of autologous and/or heterologous sheep. (A), (B), and (C) refer to three separate VMV-infected AM preparations.
[b] Aliquots of VMV-infected AMs were cultured for 7 days, and VMV titers of the last washes and day 7 supernatants were calculated.
[c] Values are expressed as the number of weeks postinstillation for a positive result to occur.

mRNA expression was observed in AMs from virus-treated lung lobes compared to that of AMs from naïve lobes ($P < 0.05$) (Fig. 3C). However, no significant difference in IL-8 expression was observed between AMs obtained from virus-treated and mock-treated lobes. No significant differences in mRNA expression of IL-1β, IL-6, IL-10, IL-12p40, IL-18, tumor necrosis factor alpha, or tumor growth factor β1 were observed between AMs from VMV-treated and mock-treated or naïve lobes. An analysis of cytokine gene expression in pretreatment AM samples and posttreatment lung tissue did not identify any significant differences between virus-treated and control lung lobes (data not shown).

Total BAL cell numbers were within normal limits for all pre- and posttreatment samples, and no significant differences in total cell numbers were observed between lung lobes. The percentages of lymphocytes within posttreatment BAL samples were significantly increased ($P < 0.05$) in BAL samples from VMV-treated lung lobes compared to those of BAL samples from posttreatment mock-treated and naïve lung lobes, and they were above normal limits (13.6% ± 4.7% [means ± standard deviations]; normal limits, 3.1% ± 2.0%). The percentages of all other cell types in posttreatment BAL samples and all cell types in pretreatment BAL samples were within normal limits, with no significant differences observed between lobes.

No significant histopathological changes were identified in any lung lobe evaluated. Immunocytochemical analysis of lung tissue failed to identify any significant differences in the numbers of airway or parenchymal major histocompatibility complex class II^+, $CD1b^+$, $CD4^+$, $CD8^+$, or $CD14^+$ cells between virus-treated, mock-treated, and naïve lung lobes (data not shown).

Infectivity of AM-associated VMV in vivo. To determine whether AM-associated VMV are infectious in vivo, autologous or heterologous VMV-infected AMs were instilled into either the lower lung or the upper respiratory tract of sheep, and the time taken for viremia and seroconversion to occur was recorded. For lower lung instillations, AMs were harvested from the right caudodorsal lung lobes of two donor Suffolk-cross ewes by BAL and subsequently infected with VMV ex vivo. Cells (1×10^6) were reinstilled into the left cardiac lung lobes of the two donor sheep (autologous instillation), and an identical number of cells were instilled into the same lobe of two further Suffolk-cross ewes (heterologous instillation). For upper respiratory tract instillations, AMs harvested from the right caudodorsal lung lobe of a Suffolk-cross ewe at postmortem subsequently were infected with VMV ex vivo, and 1×10^6 cells were instilled into the upper respiratory tract ($n = 2$) or left cardiac lung lobe ($n = 1$) of heterologous Suffolk-cross ewes. No virus was detected in samples of the final cell washes prior to instillation, implying that washing had removed viable cell-free VMV. To confirm the successful ex vivo infection of instilled cells, aliquots of each VMV-infected AM preparation were cultured in vitro for 1 week. VMV titers of in vitro culture supernatants 7 days postinfection ranged from 1.1×10^5 to 4.0×10^6 $TCID_{50}$/ml (Table 3), and VMV capsid protein was detected exclusively within AM-like cells from all cultures 7 days postinfection (data not shown), indicating successful ex vivo infection. All sheep were bled weekly up to 6 months postinstillation, and blood samples were analyzed for the presence of VMV provirus and anti-VMV antibodies.

The times taken for viremia and seroconversion to occur for each instillation are summarized in Table 3. Lower lung instillation of autologous VMV-infected AMs resulted in the detection of provirus at 2 weeks postinstillation and seroconversion at 2 to 7 weeks postinstillation. Lower lung instillation of heterologous VMV-infected AMs resulted in the detection of provirus at 2 to 11 weeks postinstillation (mean, 3.6 weeks) and seroconversion at 3 to 17 weeks postinstillation (mean, 7.6 weeks). The same heterologous VMV-infected AM preparation that resulted in successful infection after lower lung instillation failed to result in viremia or seroconversion following upper respiratory tract instillation by 6 months postinstillation. Thus, both autologous and heterologous VMV-infected AMs are infectious in vivo after lower lung instillation. The infectivity of VMV-infected AMs after upper respiratory tract instillation was not demonstrated.

Tracking of VMV-infected AMs after lower lung instillation. The presence of provirus in blood cells following lung instillation of VMV-infected AMs indicated that virus was transferred from AMs in the lung airspace into the body. The mechanism of this virus transfer is unclear. However, it is likely that virus entry involves the infection of draining lymph nodes, which are thought to be an important site of initial infection prior to dissemination throughout the body via the blood (5).

To determine whether VMV transfer from lung airspace to

TABLE 4. Postmortem analysis for the presence of PKH26-labeled cells and VMV provirus following lower lung instillation of autologous and heterologous VMV-infected, PKH26-labeled bronchoalveolar cells[a]

Sheep no.	Bronchoalveolar cell instillation type	Total BAL cell count (cells/ml lavage fluid) at:		% BAL cells PKH26$^+$ at:		BAL cell proviral DNA PCR by lobe type		Lymph node proviral DNA PCR result		
		24 h p.i.	8 days p.i.	24 h p.i.	8 days p.i.	Instilled	Naïve	Tracheobronchial	Mediastinal	Popliteal
1680	Autologous	1.4×10^7	1.6×10^7	0.91	1.16	ND	ND	ND	ND	ND
W48	Autologous	2.5×10^6	2.0×10^6	1.18	0.95	+	−	+	−	−
1103D	Autologous	ND	1.4×10^6	ND	1.38	+	−	+	−	−
817D	Autologous	ND	5.8×10^5	ND	2.45	+	−	−	−	−
O61	Heterologous	1.0×10^6	1.2×10^6	1.22	1.71	+	−	−	−	−
1102D	Heterologous	ND	4.7×10^5	ND	2.48	+	−	+	−	−
847D	Heterologous	ND	2.6×10^5	ND	2.38	+	−	−	−	−

[a] PCRs were performed to detect VMV *gag* proviral DNA. p.i., postinstillation; ND, not done.

draining lymph nodes is mediated by the direct migration of virus-infected AMs, ex vivo-infected AMs harvested from the right caudodorsal lung lobes of four donor Suffolk-cross sheep were labeled with the fluorescent dye PHK26. Labeled and infected cells (1×10^6; 88 to 93% AMs) subsequently were reinstilled into the airspace of the left cardiac lung lobes of the four donor sheep (autologous instillations) and another three Suffolk-cross sheep (heterologous instillations). To allow for analysis at an additional time point, cell instillations were performed 7 days later in three of the seven sheep (two autologous and one heterologous instillation), with cells (91 to 94% AMs) for the second instillations harvested from the left caudodorsal lung lobe and instilled into the right cardiac lung lobe.

Postmortems were performed on sheep 8 days after the first instillation, and the locations of PKH26-labeled cells within the lung and draining lymph nodes (tracheobronchial and mediastinal) were determined using fluorescence microscopy. This protocol therefore allowed the tracking of labeled AMs at 8 days postinstillation in all sheep and in three sheep at both 24 h and 8 days postinstillation. A naïve lung lobe (left caudodorsal) and a nondraining lymph node (popliteal lymph node) from each sheep were analyzed in parallel as negative controls. A cytological analysis of BAL cell populations was performed, and samples from six of seven sheep were analyzed for the presence of VMV using snPCR and immunocytochemistry. Postmortem PBMCs and serum samples were analyzed for the presence of provirus and VMV-specific antibodies by snPCR and ELISA, respectively.

The results are summarized in Table 4. Total numbers of cells ranged from 2.6×10^5 to 1.6×10^7 cells/ml BAL fluid, and results of differential cytology were within normal limits for all BAL samples (data not shown). For the three sheep instilled at two separate time points, cell numbers in 24-h- and 8-day-postinstillation BAL samples were similar for individual sheep. This suggested that no significant cell recruitment had occurred into the bronchoalveolar compartments postinstillation and that the percentage of PKH26$^+$ cells within 24-h and 8-day BAL cell populations could be compared directly. Positive cells were detected in all postinstillation BAL samples by fluorescence microscopy and generally exhibited typical AM morphology (Fig. 4A, B). No differences in the distribution or intensity of fluorescence staining of positive cells were observed between 24-h-postinstillation samples, 8-day-postinstillation samples, or stained cells prior to instillation. The percentage of PKH26$^+$ cells within BAL cell populations ranged from 0.9 to 2.5%, and the percentages of PKH26$^+$ cells within 24-h- and 8-day-postinstillation BAL samples were similar for individual sheep (Table 4). PKH26$^+$ cells were present in lung tissue sections and were located within the alveolar airspaces or within the lumen of small and large bronchioles (Fig. 4C, D). No PKH26$^+$ cells were seen in negative control lung lobes or in any of the lymph nodes, and no differences in the number or location of PKH26$^+$ cells were detected between autologous and heterologous instillations. In a further attempt to identify PKH26-labeled cells within the draining lymph nodes, fluorescence-activated cell sorting was performed on the disaggregated lymph nodes of sheep W48 and O61 to identify highly fluorescent cells of the same size and complexity as AMs. An analysis of 3×10^6 cells from each lymph node failed to identify any positively labeled cells (data not shown).

The results of snPCR analysis of BAL samples and lymph nodes also are shown in Table 4. VMV provirus was detected in BAL samples from instilled lung lobes but not from negative control lung lobes. Proviral *gag* DNA was detected in the tracheobronchial lymph nodes of two out of three sheep instilled with autologous AMs and one of three sheep instilled with heterologous AMs, but not in mediastinal or the popliteal lymph nodes. Immunocytochemical analysis for VMV capsid protein was negative for all lung tissue, lymph nodes, and BAL cells (not shown). No proviral DNA was detected in postmortem PBMC samples, and no VMV-specific antibodies were detected in postmortem serum samples.

These results indicate that virus was transferred from infected AMs within the airspace to the tracheobronchial lymph nodes within the first 8 days postinstillation. Furthermore, there was no evidence that infected AMs migrated from the airspace to the draining lymph nodes within this time period, suggesting that this transfer of virus occurred independently of direct cell migration.

DISCUSSION

In this study, it was shown that AMs are capable of the uptake of cell-free VMV after lower lung instillation in vivo. Furthermore, it was demonstrated that autologous VMV-infected AMs are capable of efficiently transmitting virus from

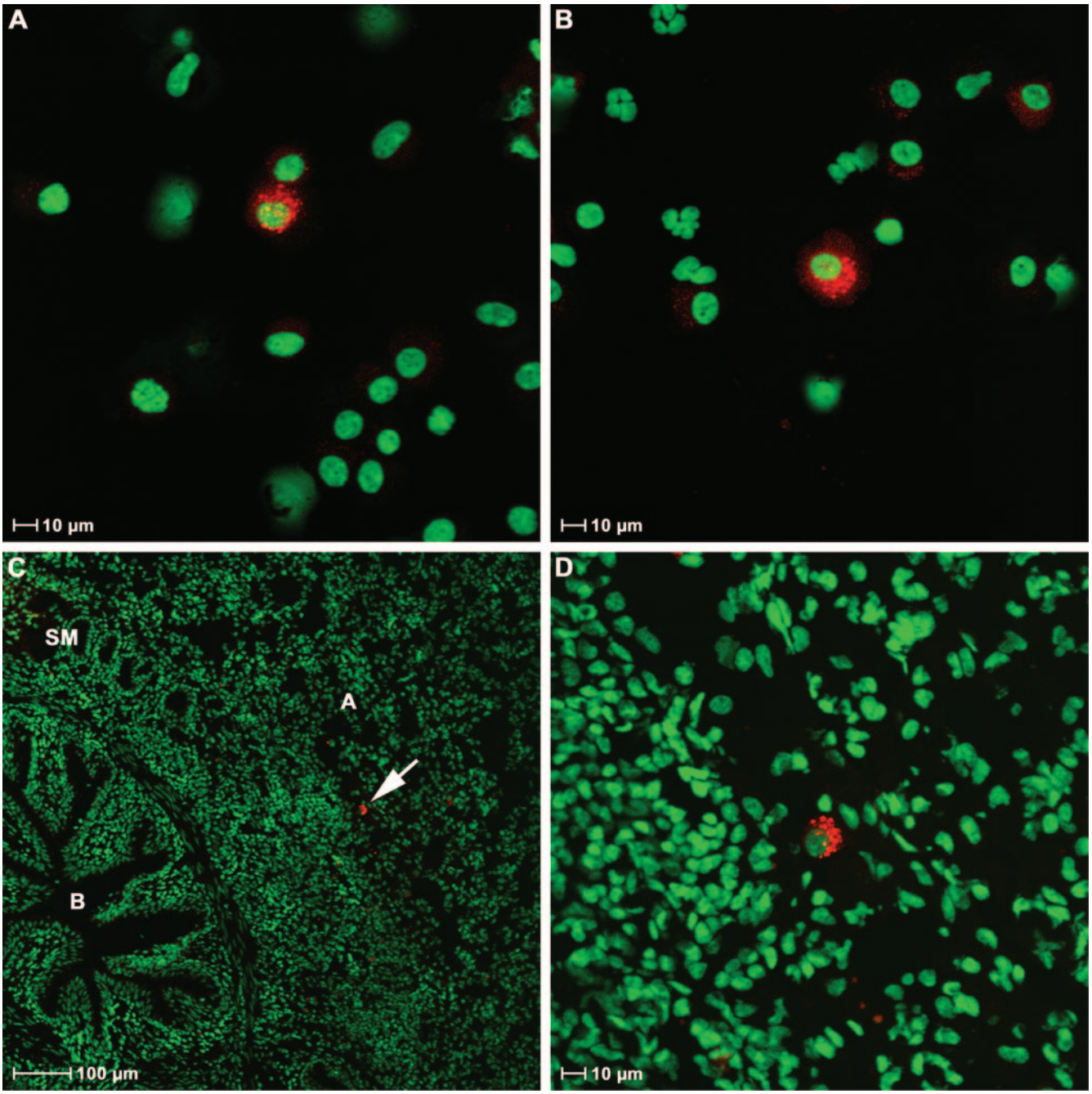

FIG. 4. Representative images of BAL cells and lung tissue from sheep W48 after instillation of autologous VMV-infected PKH26-labeled BAL cells into the lower lung. Cell nuclei were counterstained with SYBR green dye. (A) BAL cells demonstrating a $PKH26^+$ cell with AM-like morphology 8 days postinstillation. (B) BAL cells demonstrating a $PKH26^+$ cell with AM-like morphology 24 h postinstillation. (C) A single $PKH26^+$ cell (arrow) present within the alveolar region of the lung 8 days postinstillation. (D) High-power view of the $PKH26^+$ cell seen in panel C. B, bronchiole; SM, submucosal gland; A, alveolar space.

the bronchoalveolar space into the body. We have previously shown that a primary mechanism of respiratory transmission of VMV likely involves the inhalation of cell-free VMV and subsequent virus uptake in the lower lung (33). Therefore, it is possible that the uptake of VMV by resident AMs and the subsequent transfer of virus into the body represent an important route of natural respiratory transmission.

The observation that heterologous VMV-infected AMs are capable of transmitting VMV demonstrates for the first time that VMV-infected cells originating from one sheep are capable of infecting another. This was demonstrated only after lower lung instillation of infected cells, suggesting that the upper respiratory tract is relatively insensitive to cell-associated VMV, as is the case for cell-free VMV (46). As the site of particle deposition in the lung is related to particle size, with larger particles (>10 μm) being preferentially deposited in the

upper respiratory tract and only smaller particles (<5 μm) gaining access to the lower airways (20), it is likely that the majority of inhaled AMs (with average diameters of around 25 μm) would be deposited in the upper respiratory tract. However, as it has been demonstrated that a small percentage of larger particles (20 to 30 μm) may penetrate the peripheral areas of the lung (13), it is possible that a small number of inhaled AMs indeed reach the lower lung and subsequently transmit infection. Given the high efficiency of infection following lung instillation of infected AMs demonstrated here, it is possible that a relatively small number of infected AMs could transmit infection. Therefore, the transmission of VMV via the inhalation of infected AMs derived from VMV-infected sheep may represent an additional mechanism of VMV respiratory transmission. Furthermore, as VMV-infected AMs have been identified in the lungs of sheep with no VMV-induced lesions and/or no clinical signs (48), AM-associated virus transmission may represent a mechanism of transmission during early prelesional and preclinical maedi.

The tracking of fluorescently labeled VMV-infected BAL cells after lower lung instillation failed to demonstrate the migration of labeled cells from the bronchoalveolar space up to 8 days postinstillation. Evidence for a lack of cell migration from the lung airspace to the draining lymph nodes was based on two observations. First, labeled cells were not detected within the lung interstitium or lymph nodes. Second, the percentages of positively labeled cells in BAL samples were similar at both 24 h and 8 days postinstillation. The intensity and distribution of the staining of labeled cells at both time points were identical to those of the stained cells preinstillation; this indicated that positive cells detected within the lung airspace had not proliferated within the lung airspace or had been phagocytosed by other resident macrophages. This, therefore, allowed a direct comparison of positive cell counts between samples from the 24-h and 8-day time points, which, given their similarities, suggests that no migration from the airspace had occurred between these two time points. However, we cannot rule out the possibility that some labeled cells migrated immediately (<24 h) after instillation, or that a small number of labeled cells migrated to the lymph node but remained undetected.

Analysis for VMV identified proviral DNA but not viral protein within labeled cell populations, indicating a typical in vivo-restricted pattern of replication (19, 22), and demonstrated provirus within the tracheobronchial lymph nodes of sheep 8 days after instillation of both autologous and heterologous VMV-infected AMs. Provirus was present in the draining lymph node at a time comparable to that of a previous study of cell-free VMV transfer from skin to draining lymph nodes, which detected VMV-infected cells within the lymph node from 4 days postinfection, with maximum numbers seen between days 7 and 14 (5). The lack of evidence for direct cell migration of VMV-infected AMs to this lymph node suggests that virus transport from AMs to the tracheobronchial lymph node occurred via an intermediate route and not by direct cell migration of VMV-infected AMs. There did not appear to be any significant difference in the dynamics of virus transfer to the lymph nodes following instillation of either autologous or heterologous AMs, and this was consistent with our observation that, following instillation of either autologous or heterologous VMV-infected AMs, viremia and seroconversion occur at similar time points.

Transfer of virus from AMs to the tracheobronchial lymph node could occur in two ways. First, cell-free virus particles may be released from infected AMs, gain access to the lung interstitium, and travel directly via the afferent lymph to the draining lymph node. Second, VMV may be transferred from AMs to an intermediate cell type that subsequently migrates to the lymph node. A previous study of initial VMV dissemination after intradermal inoculation suggested that of these two possibilities, virus transfer via an intermediate cell type rather than as free virus is most likely: an analysis of afferent lymph draining the virus inoculation sites demonstrated that virus was exclusively cell associated, with no evidence of cell-free VMV within lymph plasma (36). Furthermore, these VMV-positive cells were shown to be afferent lymph DCs, suggesting that respiratory tract DCs (RTDCs), which are found adjacent to airways in high numbers (32), play a similar role in virus transfer in the lung.

Both of these mechanisms would require the AMs to be productively infected. The present study found evidence for VMV *gag*, *rev*, and *env* transcript production in AMs following free virus administration and provirus DNA in ex vivo-infected AMs. In contrast, no virus protein could be detected by immunocytochemistry in either case, indicating that the virus in AMs exhibited a typical in vivo-restricted pattern of replication (22). However, due to a relative lack of sensitivity of the immunocytochemical technique, a small but significant number of AMs may have been productively infected but remained undetected.

Interestingly, PCR analysis of in vivo-infected AMs detected two populations of *env* gene transcripts generated by alternative splicing, whereas only the smaller *env* gene transcript was detected in in vitro-infected OSCs. As the two *env* transcripts differed by an insert 5′ to the start of translation, the functional significance of this alternative splicing event is unclear, as it would be expected to have no effect on the structure of the translated protein. However, the absence of the larger *env* transcripts in productively infected OSCs indicates that in these cells at least, the additional 45-bp insert is not required for productive virus replication.

We hypothesized that VMV induces inflammatory responses during initial infection, which subsequently would enhance virus uptake, either by the recruitment of VMV target cells, e.g., RTDCs, or by dysregulation of cytokine gene expression and subsequent enhancement of VMV replication. Therefore, a detailed analysis of lung inflammatory responses during early infection with VMV strain EV1 was undertaken. Up-regulation of AM GM-CSF mRNA expression was observed 7 days after endoscopic instillation of VMV. This finding is consistent with those of previous studies of naturally infected sheep lungs, which demonstrated up-regulation of AM GM-CSF expression in combination with up-regulation of other proinflammatory cytokines and/or observable lung inflammation (29, 50). AM IL-8 mRNA expression also was increased in virus-treated lung lobes compared to that of untreated lung lobes but not compared to that of mock-treated lobes, suggesting that the IL-8 response either was due to the BAL procedure or was induced by components of the tissue culture medium of virus and mock virus instillates. No changes in AM expression of other proin-

flammatory cytokines were observed in this study, and with the exception of an increase in bronchoalveolar lymphocyte populations, analysis of lung tissue failed to demonstrate evidence of lung inflammation. This is in contrast to two previous reports of endoscopic instillation of VMV, which identified extensive inflammatory changes in virus-treated lung lobes after 11 days postinfection (17, 42). However, in these studies, higher doses of a different strain of virus were used and the sheep were of a different breed, each of which could influence the degree of inflammatory response.

The observations in this study suggest that up-regulation of AM GM-CSF mRNA expression was a specific effect of VMV infection and was not due to the BAL procedure or the tissue culture medium and was not secondary to a generalized inflammatory response. Furthermore, as virus infection after the instillation of cell-free VMV strain EV1 into the lower lung is known to be highly efficient (33), these results suggest that a generalized inflammatory response is not essential for VMV uptake in the lung. The mechanism(s) by which VMV up-regulates AM GM-CSF expression in the absence of inflammation is unclear, although interestingly, up-regulation of this cytokine has been demonstrated in in vitro-cultured AMs in response to inactivated VMV, suggesting that the interaction between virus components and cell surface receptors is sufficient for GM-CSF induction (49).

The specific increase in bronchoalveloar lymphocyte numbers following VMV instillation is consistent with findings of previous experimental infection studies (2, 8) and, as lymphocyte infiltration is a characteristic of lymphoid interstitial pneumonia, may represent the early stages of VMV-induced pneumonia. How this lymphocyte recruitment is mediated is unclear, but GM-CSF may be involved. It is known that local T-cell responses within the lung are down-regulated by resident AMs (43, 45) and that GM-CSF is capable of abrogating this immunosuppressive activity (3). Therefore, local GM-CSF production by AMs may result in increased T-cell responses within the bronchoalveolar space, with a resultant increase in lymphocyte numbers. This would be consistent with the observation that GM-CSF appears to be a key driver in lung lesion development in naturally infected sheep (49, 50).

In addition to playing a potential role in the pathogenesis of lymphoid interstitial pneumonia, up-regulation of GM-CSF expression by AMs in the early stages of infection also may have implications regarding the initial uptake of VMV in the lung. First, it has been demonstrated that GM-CSF enhances VMV replication in monocyte-derived macrophages in vitro (50). If a similar enhancement occurs in pulmonary macrophages, this could result in increased virus levels within the lung and subsequently may increase virus uptake. Second, as previously discussed, virus uptake from the lung airspace is likely to involve RTDCs. Under steady-state conditions, AMs maintain RTDCs in a down-modulated state (24). Treatment with GM-CSF has been shown to inhibit this immunosuppressive activity (3, 4). In addition, GM-CSF has been shown to directly up-regulate the antigen-presenting activity of RTDCs (1, 10) and also has been implicated in RTDC recruitment (44, 47). Therefore, the up-regulation of GM-CSF expression in AMs may result in the switching of RTDCs toward a more activated phenotype and also recruit RTDCs toward virus-infected AMs, potentially enhancing RTDC uptake of virus within the lung.

Furthermore, it is known that cellular interactions between DCs and $CD4^+$ T cells within the draining lymph nodes are crucial for VMV transfer from DCs to macrophages, which are thought to be the main disseminator of VMV around the body (16). Therefore, increased activation of RTDCs may result in increased DC-$CD4^+$ T-cell interactions within the lymph nodes with the subsequent enhancement of virus transfer to macrophages. This may in turn lead to increased viral dissemination throughout the body.

In conclusion, this study has demonstrated that resident AM populations within the lung are capable of the uptake of cell-free VMV and that this results in a specific up-regulation of AM GM-CSF expression, which may in turn facilitate virus uptake in the lower lung. Infected AMs were shown to be capable of transmitting virus from the lower lung airspace, but not from the upper respiratory tract, into the body. Furthermore, this transfer of virus did not appear to be mediated by direct cell migration but appeared to involve an intermediate route.

ACKNOWLEDGMENTS

Tom McNeilly was supported by a Ph.D. studentship from the Royal (Dick) College of Veterinary Studies, University of Edinburgh, and by funding from the European Union (contract no. QLK2-CT-2002-00167).

We thank Peter Tennant for technical assistance during the in vivo infection studies, Shonna Johnston for assistance with fluorescence-activated cell sorter analysis, and Paul Wright for his excellent care of the experimental animals during this study. We also thank John Hopkins (University of Edinburgh) and Ian Anderson (Moredun Research Institute) for the kind provision of monoclonal antibodies.

REFERENCES

1. **Armstrong, L. R., P. J. Christensen, R. Paine III, G. H. Chen, R. A. McDonald, T. K. Lim, and G. B. Toews.** 1994. Regulation of the immunostimulatory activity of rat pulmonary interstitial dendritic cells by cell-cell interactions and cytokines. Am. J. Respir. Cell Mol. Biol. **11:**682–691.
2. **Begara, I., L. Lujan, D. D. Collie, H. R. Miller, and N. J. Watt.** 1996. Early pulmonary cell response during experimental maedi-visna virus infection. Vet. Immunol. Immunopathol. **55:**115–126.
3. **Bilyk, N., and P. G. Holt.** 1995. Cytokine modulation of the immunosuppressive phenotype of pulmonary alveolar macrophage populations. Immunology **86:**231–237.
4. **Bilyk, N., and P. G. Holt.** 1993. Inhibition of the immunosuppressive activity of resident pulmonary alveolar macrophages by granulocyte/macrophage colony-stimulating factor. J. Exp. Med. **177:**1773–1777.
5. **Blacklaws, B., P. Bird, and I. McConnell.** 1995. Early events in infection of lymphoid tissue by a lentivirus, maedi-visna. Trends Microbiol. **3:**434–440.
6. **Blacklaws, B. A., E. Berriatua, S. Torsteinsdottir, N. J. Watt, A. D. de Klein, and G. D. Harkiss.** 2004. Transmission of small ruminant lentiviruses. Vet. Microbiol. **101:**199–208.
7. **Brodie, S. J., L. D. Pearson, M. C. Zink, H. M. Bickle, B. C. Anderson, K. A. Marcom, and J. C. DeMartini.** 1995. Ovine lentivirus expression and disease. Virus replication, but not entry, is restricted to macrophages of specific tissues. Am. J. Pathol. **146:**250–263.
8. **Cadoré, J. L., F. Guiguen, G. Cordier, R. Loire, M. Lyon, J. Chastang, T. Greenland, Court-Fortune, D. Revel, and J. F. Mornex.** 1993. Early events in the experimental interstitial lung disease induced in sheep by the Visna-maedi virus. Immunol. Lett. **39:**39–43.
9. **Carrozza, M. L., M. Mazzei, P. Bandecchi, M. Arispici, and F. Tolari.** 2003. In situ PCR-associated immunohistochemistry identifies cell types harbouring the Maedi-Visna virus genome in tissue sections of sheep infected naturally. J. Virol. Methods **107:**121–127.
10. **Christensen, P. J., L. R. Armstrong, J. J. Fak, G. H. Chen, R. A. McDonald, G. B. Toews, and R. Paine III.** 1995. Regulation of rat pulmonary dendritic cell immunostimulatory activity by alveolar epithelial cell-derived granulocyte macrophage colony-stimulating factor. Am. J. Respir. Cell Mol. Biol. **13:**426–433.
11. **Collie, D. D., A. Baker, S. Mauchline, D. Porteous, and G. McLachlan.** 1999.

Ovine bronchoalveolar lavage cellularity: reproducibility and the effect of multiple repeated lavage. Res. Vet. Sci. **67:**137–140.
12. **Corry, D., P. Kulkarni, and M. F. Lipscomb.** 1984. The migration of bronchoalveolar macrophages into hilar lymph nodes. Am. J. Pathol. **115:**321–328.
13. **Driessen, M. N., and P. H. Quanjer.** 1991. Pollen deposition in intrathoracic airways. Eur. Respir. J. **4:**359–363.
14. **Egan, P. J., W. Kimpton, H. F. Seow, V. M. Bowles, M. R. Brandon, and A. D. Nash.** 1996. Inflammation-induced changes in the phenotype and cytokine profile of cells migrating through skin and afferent lymph. Immunology **89:**539–546.
15. **Ellis, J. A., H. I. Russell, and C. W. Du.** 1994. Effect of selected cytokines on the replication of Corynebacterium pseudotuberculosis and ovine lentiviruses in pulmonary macrophages. Vet. Immunol. Immunopathol. **40:**31–47.
16. **Eriksson, K., E. McInnes, S. Ryan, P. Tonks, I. McConnell, and B. Blacklaws.** 1999. $CD4^+$ T-cells are required for the establishment of maedi-visna virus infection in macrophages but not dendritic cells in vivo. Virology **258:**355–364.
17. **Geballe, A. P., P. Ventura, L. Stowring, and A. T. Haase.** 1985. Quantitative analysis of visna virus replication in vivo. Virology **141:**148–154.
18. **Gelmetti, D., L. Gibelli, E. Brocchi, and G. Cammarata.** 2000. Using a panel of monoclonal antibodies to detect Maedi virus (MV) in chronic pulmonary distress of sheep. J. Virol. Methods **88:**9–14.
19. **Gendelman, H. E., O. Narayan, S. Molineaux, J. E. Clements, and Z. Ghotbi.** 1985. Slow, persistent replication of lentiviruses: role of tissue macrophages and macrophage precursors in bone marrow. Proc. Natl. Acad. Sci. USA **82:**7086–7090.
20. **Gordon, S. B., and R. C. Read.** 2002. Macrophage defences against respiratory tract infections. Br. Med. Bull. **61:**45–61.
21. **Gupta, V. K., I. McConnell, R. G. Dalziel, and J. Hopkins.** 1996. Identification of the sheep homologue of the monocyte cell surface molecule CD14. Vet. Immunol. Immunopathol. **51:**89–99.
22. **Haase, A. T., L. Stowring, P. Narayan, D. Griffin, and D. Price.** 1977. Slow persistent infection caused by visna virus: role of host restriction. Science **195:**175–177.
23. **Harmsen, A. G., B. A. Muggenburg, M. B. Snipes, and D. E. Bice.** 1985. The role of macrophages in particle translocation from lungs to lymph nodes. Science **230:**1277–1280.
24. **Holt, P. G., J. Oliver, N. Bilyk, C. McMenamin, P. G. McMenamin, G. Kraal, and T. Thepen.** 1993. Downregulation of the antigen presenting cell function(s) of pulmonary dendritic cells in vivo by resident alveolar macrophages. J. Exp. Med. **177:**397–407.
25. **Hopkins, J., B. M. Dutia, and I. McConnell.** 1986. Monoclonal antibodies to sheep lymphocytes. I. Identification of MHC class II molecules on lymphoid tissue and changes in the level of class II expression on lymph-borne cells following antigen stimulation in vivo. Immunology **59:**433–438.
26. **Howard, C. J., P. Sopp, G. Bembridge, J. Young, and K. R. Parsons.** 1993. Comparison of CD1 monoclonal antibodies on bovine cells and tissues. Vet. Immunol. Immunopathol. **39:**77–83.
27. **Johansson, A., and P. Camner.** 1980. Are alveolar macrophages translocated to the lymph nodes? Toxicology **15:**157–162.
28. **Legastelois, I., G. Cordier, G. Cozon, J. L. Cadore, F. Guiguen, T. Greenland, and J. F. Mornex.** 1996. Visna-maedi virus-induced expression of interleukin-8 gene in sheep alveolar cells following experimental in vitro and in vivo infection. Res. Virol. **147:**191–197.
29. **Legastelois, I., V. Cottin, J. F. Mornex, and G. Cordier.** 1997. Alveolar macrophages from sheep naturally infected by visna-maedi virus contribute to IL-8 production in the lung. Vet. Immunol. Immunopathol. **59:**131–139.
30. **Luján, L., I. Begara, D. Collie, and N. J. Watt.** 1994. Ovine lentivirus (maedi-visna virus) protein expression in sheep alveolar macrophages. Vet. Pathol. **31:**695–703.
31. **Maddox, J. F., C. R. Mackay, and M. R. Brandon.** 1985. Surface antigens, SBU-T4 and SBU-T8, of sheep T lymphocyte subsets defined by monoclonal antibodies. Immunology **55:**739–748.
32. **McNeilly, T. N., J. K. Brown, and G. Harkiss.** 2006. Differential expression of cell surface markers by ovine respiratory tract dendritic cells. J. Histochem. Cytochem. **54:**1021–1030.
33. **McNeilly, T. N., P. Tennant, L. Lujan, M. Perez, and G. D. Harkiss.** 2007. Differential infection efficiencies of peripheral lung and tracheal tissues in sheep infected with Visna/maedi virus via the respiratory tract. J. Gen. Virol. **88:**670–679.
34. **Pépin, M., C. Vitu, P. Russo, J. F. Mornex, and E. Peterhans.** 1998. Maedi-visna virus infection in sheep: a review. Vet. Res. **29:**341–367.
35. **Reyburn, H. T., D. J. Roy, B. A. Blacklaws, D. R. Sargan, and I. McConnell.** 1992. Expression of maedi-visna virus major core protein, p25: development of a sensitive p25 antigen detection assay. J. Virol. Methods **37:**305–320.
36. **Ryan, S., L. Tiley, I. McConnell, and B. Blacklaws.** 2000. Infection of dendritic cells by the Maedi-visna lentivirus. J. Virol. **74:**10096–10103.
37. **Saman, E., E. G. Van, L. Lujan, B. Extramiana, G. Harkiss, F. Tolari, L. Gonzalez, B. Amorena, N. Watt, and J. Badiola.** 1999. A new sensitive serological assay for detection of lentivirus infections in small ruminants. Clin. Diagn. Lab. Immunol. **6:**734–740.
38. **Sargan, D. R., I. D. Bennet, C. Cousens, D. J. Roy, B. A. Blacklaws, R. G. Dalziel, N. J. Watt, and I. McConnell.** 1991. Nucleotide sequence of EV1, a British isolate of maedi-visna virus. J. Gen. Virol. **72:**1893–1903.
39. **Sargan, D. R., D. J. Roy, R. G. Dalziel, N. J. Watt, and I. McConnell.** 1994. A temporal study of RNAs produced in maedi-visna virus infection of choroid plexus cells. Vet. Microbiol. **39:**369–378.
40. **Sigurdsson, B., H. Grimsson, and P. A. Palsson.** 1952. Maedi, a chronic, progressive infection of sheep's lungs. J. Infect. Dis. **90:**233–241.
41. **Sigurdsson, B., and P. A. Palsson.** 1958. Visna of sheep; a slow, demyelinating infection. Br. J. Exp. Pathol. **39:**519–528.
42. **Staskus, K. A., L. Couch, P. Bitterman, E. F. Retzel, M. Zupancic, J. List, and A. T. Haase.** 1991. In situ amplification of visna virus DNA in tissue sections reveals a reservoir of latently infected cells. Microb. Pathog. **11:**67–76.
43. **Strickland, D. H., T. Thepen, U. R. Kees, G. Kraal, and P. G. Holt.** 1993. Regulation of T-cell function in lung tissue by pulmonary alveolar macrophages. Immunology **80:**266–272.
44. **Tazi, A., F. Bouchonnet, M. Grandsaigne, L. Boumsell, A. J. Hance, and P. Soler.** 1993. Evidence that granulocyte macrophage-colony-stimulating factor regulates the distribution and differentiated state of dendritic cells/Langerhans cells in human lung and lung cancers. J. Clin. Investig. **91:**566–576.
45. **Thepen, T., G. Kraal, and P. G. Holt.** 1994. The role of alveolar macrophages in regulation of lung inflammation. Ann. N. Y. Acad. Sci. **725:**200–206.
46. **Torsteinsdóttir, S., S. Matthiasdottir, N. Vidarsdottir, V. Svansson, and G. Petursson.** 2003. Intratracheal inoculation as an efficient route of experimental infection with maedi-visna virus. Res. Vet. Sci. **75:**245–247.
47. **Wang, J., D. P. Snider, B. R. Hewlett, N. W. Lukacs, J. Gauldie, H. Liang, and Z. Xing.** 2000. Transgenic expression of granulocyte-macrophage colony-stimulating factor induces the differentiation and activation of a novel dendritic cell population in the lung. Blood **95:**2337–2345.
48. **Watt, N. J., N. MacIntyre, D. Collie, D. Sargan, and I. McConnell.** 1992. Phenotypic analysis of lymphocyte populations in the lungs and regional lymphoid tissue of sheep naturally infected with maedi visna virus. Clin. Exp. Immunol. **90:**204–208.
49. **Woodall, C. J., L. J. Maclaren, and N. J. Watt.** 1997. Differential levels of mRNAs for cytokines, the interleukin-2 receptor and class II DR/DQ genes in ovine interstitial pneumonia induced by maedi visna virus infection. Vet. Pathol. **34:**204–211.
50. **Zhang, Z., G. D. Harkiss, J. Hopkins, and C. J. Woodall.** 2002. Granulocyte macrophage colony stimulating factor is elevated in alveolar macrophages from sheep naturally infected with maedi-visna virus and stimulates maedi-visna virus replication in macrophages in vitro. Clin. Exp. Immunol. **129:** 240–246.